# Texture Discrimination by Local Generalized Symmetry

Y. Bonneh D. Reisfeld Y. Yeshurun

Department of Computer Science
Tel Aviv University
69978 Tel Aviv, Israel

## Abstract

*Texture consists of local variance of grey level or edge intensity values. We have recently presented a Generalized Symmetry operator, that captures local spatial relations of image patterns. We show that activity differences in the continuous intensity map produced by the local generalized symmetry operator can be efficiently used to detect texture boundaries. Using almost all available quantitative results of human performance in artificial texture discrimination, we show that our algorithm favorably compares with other computational approaches (correlation coefficient $> 0.9$ between our model's performance and available human performance). Stressing the necessity of benchmarks for Computer Vision algorithms, we construct an exhaustive set of textures that could be used as experimental stimuli for both humans and machines, and demonstrate the performance of the algorithm on some of these artificial textures as well as on natural images.*

## 1 Introduction

Humans are able to discriminate between surfaces sharing the same average color and brightness but differ in small scale luminance variations generally called texture. This ability is vital to segmentation since natural objects are often heterogeneous and their boundary cannot always be found by standard edge detectors. The classical work of Julesz claimed that texture discrimination could be explained in terms of global second order statistic differences between points in the image [8]. Later work attributed the discrimination to first-order differences in features such as orientation, size and brightness of local texture elements. [9, 11, 2, 3]. The Texton theory [9] specifies these elements as Textons, that are elongated blobs with specific color, orientation and size, line ends (terminators) and line crossings. All these theories were based on a qualitative distinction between effortless preattentive texture discrimination and the more time consuming attentive discrimination.

Recent psychophysical experiments questioned the preattentive-attentive dichotomy. They found graded discriminability in textures composed from randomly rotated patterns (similar to Figure 2) [7]. Similar results were obtained in detection tasks [12]. They provide us with a database of discriminability measures for a set of artificial pattern pairs. These observations raise the need for a computational model that discriminates between textures in a continuous manner and can be quantitatively compared with human performance.

We have recently presented a generalized symmetry measure and demonstrated its application to detection of interest points in natural images [15], and for face recognition [5] and normalization [16] tasks. The basis of our operator is the quantification of local spatial relations between image edges. This is carried out by assigning activity values to image points. Since texture is characterized by local spatial relations of image edges, we suggest a computational model that takes as an input the intensity gradient at each image point, and generates activity maps of the generalized symmetry in different scales. Areas of different texture are thus characterized by different activity on one or more of these maps.

Some recent computational models [6, 14] are also quantitative and continuous, and are compared to psychophysical data. They are based on linear filters followed by a non-linear stage and produce activity maps where the texture boundary becomes activity gradient. Comparing our model to these models, we find that our model yields a better fit to available quantitative psychophysical data.

Many computational models for texture discrimination use ad-hoc artificial examples that show the superiority of certain models to other models. We



0-8186-3870-2/93 $3.00 © 1993 IEEE

suggest a method for constructing an exhaustive set of artificial patterns that can be used as a data base for texture analysis, and demonstrate the performance of our model on some new artificial textures derived from this data base, as well as on natural images.

## 2 Generalized Symmetry

The generalized symmetry operator is described in [15] and in a slightly different formulation in [16]. We briefly sketch the version used in the current work. Let $p_k$ be any point in the input image ($k = 1, \ldots, K$). Denote $v_k = (r_k, \theta_k)$ the edge at $p_k$ such that $r_k$ is the edge magnitude and $\theta_k \in [0, \pi]$ is the edge orientation. For each two points $p_i$ and $p_j$, we denote by $\alpha_{ij}$ the counterclockwise angle between the line passing through these points and the horizon. We define the set $\Gamma(p, \psi)$, a distance weight function $D_\sigma(i, j)$, and a phase weight function $P(i, j)$ as

$$\begin{aligned} \Gamma(p,\psi) &= \left\{ (i,j) \;\middle|\; \frac{p_i + p_j}{2} = p\,,\ \frac{\theta_i + \theta_j}{2} = \psi \right\} \\ D_\sigma(i,j) &= G_\sigma(\|p_i - p_j\|) \\ P(i,j) &= G_{\sigma_0}(\theta_i - \alpha_{ij} - \pi/2)\, G_{\sigma_0}(\theta_i - \alpha_{ij} - \pi/2) \end{aligned}$$

where $G_\sigma(t) = \frac{1}{\sqrt{2\pi}\sigma} \exp -\frac{t}{2\sigma}$ is the Gaussian. The phase tuning $\sigma_0$ is fixed. $\sigma$ of $D_\sigma$ corresponds to a locality channel.

The symmetry measure $S_\sigma(p, \psi)$ at point $p$ in direction $\psi$ is defined as

$$S_\sigma(p,\psi) = \sum_{(i,j)\in\Gamma(p,\psi)} D_\sigma(i,j) P(i,j) r_i r_j$$

Let $\gamma$ be such that $S_\sigma(p, \gamma)$ is maximal and $I_\gamma = [\gamma - \pi/4, \gamma + \pi/4)$ an interval around $\gamma$. The *Radial Symmetry* is defined as

$$RS_\sigma(p) = \int_{\psi\in I_\gamma} (1 + S_\sigma(p,\psi))d\psi \int_{\psi\notin I_\gamma} (1 + S_\sigma(p,\psi))d\psi$$

These definitions quantify the symmetry at each point $p$, by summing the support of each two edge points $p_i, p_j$ such that $p = \frac{p_i + p_j}{2}$. When the edges are of the same orientation there is no support for symmetry. The strongest support is when the two edge orientations are both orthogonal to the virtual line connecting the points. The phase function is monotonic between these two extreme cases. In addition, the operator is local due to the locality weighting function where $\sigma$ determines the locality channel.

Isotropic symmetry at point $p$ is defined as the sum of all symmetry values at $p$. The Radial Symmetry

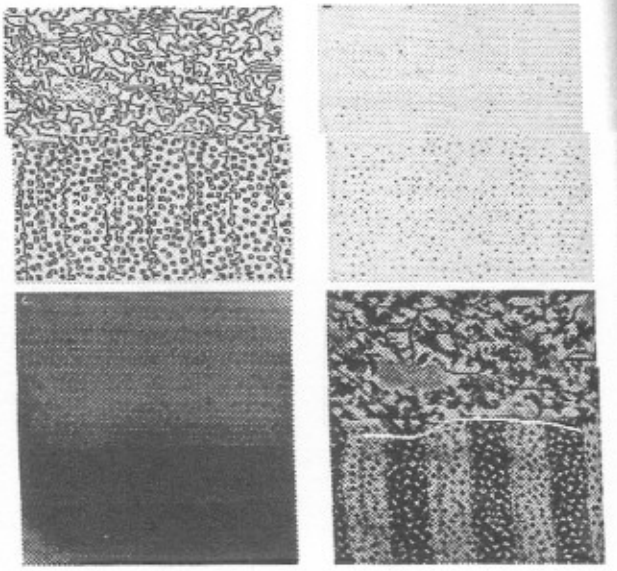

Figure 1: Application of the model to natural texture. From top to bottom left to right: Edge map, Computed symmetry maps, Blur of the symmetry map, Low frequency edges of the symmetry map superimposed on the original image

$RS_\sigma(p)$ is identical to the isotropic symmetry when there is only one prominent symmetry direction at $p$, which is the common case. However, closed figures, especially a circle, induce symmetry at various orientations at their center point and give rise to higher radial symmetry values.

## 3 Texture Discrimination

We discriminate textures by using symmetry maps: Following edge detection, the radial symmetry is computed in a number of maps, each corresponding to a different locality parameter $\sigma$. Texture boundaries are located at high gradient locations in one of these maps and computed by a low frequency edge detector.

Figure 1 demonstrates natural texture discrimination. Consider the demonstration in the left column. The texture is composed of two cloth sheets coded in a 270 × 270 pixels image. The horizontal boundary between the two clothes is clearly visible, but the discrimination is not trivial, since there is no difference in average intensity or in busyness (absolute value of the Laplacian of Gaussian). The first edge detection stage,(top left), is implemented with a set of 8 even oriented Gabor filters (7 × 7 pixels in size, $\omega = 0.6$ , $\sigma = 3$) followed by rectification (threshold at 0) yield-

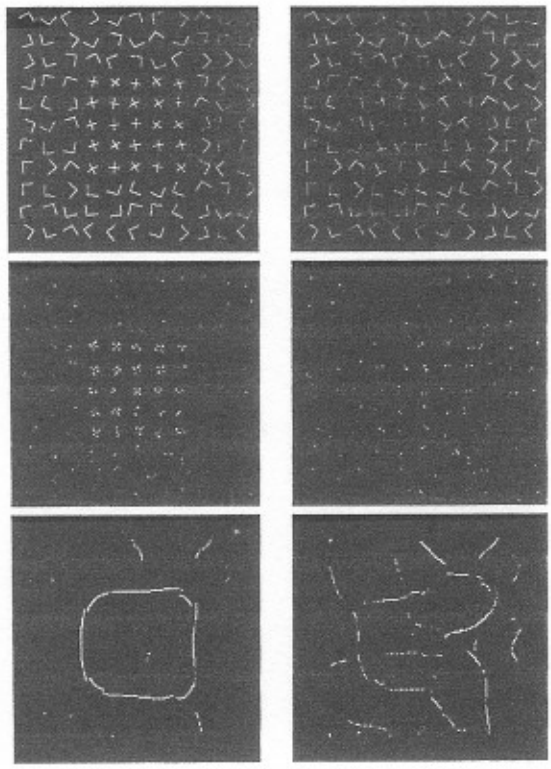

Figure 2: Artificial texture discrimination by the model. Top raw - the textures, middle - local symmetry maps, bottom - computed boundaries.

ing 8 filtered images. At each point, the filter with the strongest response is selected as the edge magnitude and its orientation as the edge orientation. This stage is followed by a non-maxima suppression process for edge thinning. We have used this simple method because it is a coarse approximation to oriented simple cells. Other methods were tested with equal success. The responses of the radial symmetry (top right) were obtained using $\sigma = 1$. The difference in the symmetry response is clearly seen. Finally, the texture boundary becomes explicit by the gradient of symmetry (marked on the original image). Other similar natural textures were discriminated by the model with equal success.

The discrimination of artificial textures widely studied in psychophysical experiments is described in the following section.

## 4 Psychophysical Correlates

Almost all psychophysical studies of texture discrimination use artificial textures of various types and test their discriminability. The most popular paradigm uses split fields of randomly rotated micro patterns. Figure 2 demonstrates the model's operation on such artificial textures. The top and middle rows demonstrate textures composed from X-L and L-T patterns. These textures are widely studied [10, 7, 12, 6, 14, 4] based on the fact that the X-L texture is easily discriminated while the L-T requires more time and attention. This was measured (among other pattern pairs) by Gurnsey and Browse [7] and in equivalent detection tasks by Krose [12]. The current explanations include the Texton theory [9] that attributes the X-L discrimination to a crossing texton, the size-tuning principle [4] that attributes discrimination to different in size, and models that define filter mechanisms producing the desired results [6, 14]. Our model gives an intuitive explanation to these examples. The symmetry response for the X pattern has four components, the T has two and the L one, where all symmetries are identical when applied locally. If discriminability is attributed to difference in total symmetry, then X-L should discriminate much easier than the L-T. We applied our model to these textures using the same edge detection stages as used for the natural textures with local symmetry computation ($\sigma = 2$). The computed symmetry maps are displayed in Figure 2 middle raw while the explicit boundary in the bottom raw. The boundary of the X-L texture is clearly visible (bottom left) while the boundary of the L-T texture is not clear although some fragments of it can be noticed. We applied this procedure successfully to other artificial textures including patterns that are not made of small liine segments (e.g. circle).

It is important to note that the discrimination of these artificial textures is a simple task and can be done in many different ways. The key point is not to discriminate these textures, but to match human performance in texture discrimination.

In order to compare our model to human performance, we define a discriminability measure between micro-pattern pairs. The symmetry measure for a micro-pattern $m$, which is a small binary image, is the sum of the radial symmetry of all its points:

$$S_\sigma(m) = \sum_{p \in m} RS_\sigma(p)$$

The discriminability measure between two micro-patterns $m1$ and $m2$ in a channel determined by $\sigma$ is defined as

$$D_\sigma(m1, m2) = log(S_\sigma(m1)) - log(S_\sigma(m2))$$

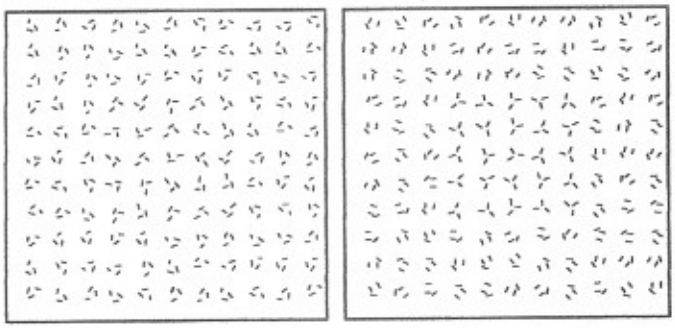

Figure 4: Randomly generated 3 line pattern textures. Left - similar second oreder statistics, relatively strong discriminability predicted. Right - weak discriminability predicted

The (total) discriminability is

$$D(m1, m2) = \max_{\sigma}(D_{\sigma}(m1, m2))$$

which is the maximal response over all channels. This is a natural extension to models of brightness perception (e.g [13]), since the luminance and the symmetry edges might be computed the same way. We applied this computation to the patterns studied by Gurnsey & Browse [7] using $30 \times 30$ pixels patterns, 2 channels with $\sigma_d = 7$ and 40 pixels and $\sigma_0 = 0.125$. Results appear in Figure 3. The black bars represent human discrimination power, where higher value stands for easier discrimination. The grey bars represent the model's discriminability values after linear regression. The computed correlation is $\rho = 0.92$. We applied the same procedure to data from Krose [12] and received correlation of $\rho = 0.86$ and $\rho = 0.98$ for his two experiments. These values are better than those reported previously [6, 12].

## 5 Discussion

We have treated texture discrimination as a continuous phenomena and developed a model based on generalized symmetry which shows good correlation with psychophysical data.

The symmetry operator is local, as expressed in its distance weight function. Therefore, one may suspect that locality per se is sufficient, since discrimination may be merely based on evaluating the size of the micro-patterns and comparing it for both textures [4]. Bergen & Adelson [4] demonstrated this principle using the rectified Laplacian of Gaussian. We have tested a variant of the symmetry model, which stress this locality idea, by neglecting the phase component. This decreases the correlation to the psychophysical data to 0.73 instead of 0.92 that the full model achieves. This degradation is mainly due to micro-patterns with identical second order statistics like pair 3.1 in Figure 3.

Next we consider the biological plausibility of our model. Since it involves a non-recurrent parallel computation, it can clearly be realized in cortical circuits. A cortical implementation may involve local, intra columnar connections, as well as interactions between hyper-columns that can integrate the symmetry over small segments of the image. This may correspond to the evidence on cortical cells in V1 whose response is modulated by stimulus beyond the classical receptive fields [1]. A different approach involves a specific cortical mechanism that can detect co-circularity of edges based on local support ([18]). Using the same mechanism that detects co-circularity with different synaptic weights will detect local symmetry.

The asymmetry of figure-ground in texture discrimination is found in [7] and in similar detection tasks in [19] and is also addressed in [17]. For example, it is easier to detect a square of L patterns embedded in surrounding X patterns than vise versa. In testing our model, we have used the reported average discriminability as done by others [14, 6]. Assuming that patterns with lower symmetry value are more easily detected (e.g Ls among Xs), our model can account for about 70% of the cases in the psychophysical database. It is possible that a somewhat different formulation of the generalized symmetry might account for all cases and is left for further study.

Next we would like to point out that the set of patterns used in texture psychophysics is highly skewed. Most of it was constructed in order to demonstrate a specific principle or theory. Therefore, it is possible that these patterns, that are traditionally used as test data, are not sufficient for the purpose of assessing new algorithms and theories. We have therefore constructed a data base of $10^4$ micro-patterns by generating patterns composed of three line segments whose position is selected at random (see Figure 4). This might be the first step towards constructing a large data base of artificial textures that could be used for evaluating computational models for texture discrimination.

We hypothesized that patterns that differ in their generalized symmetry will be easily discriminated by humans and vice versa, and used textures from this data base in order to verify it. In order to exclude other factors, like differences in the second order

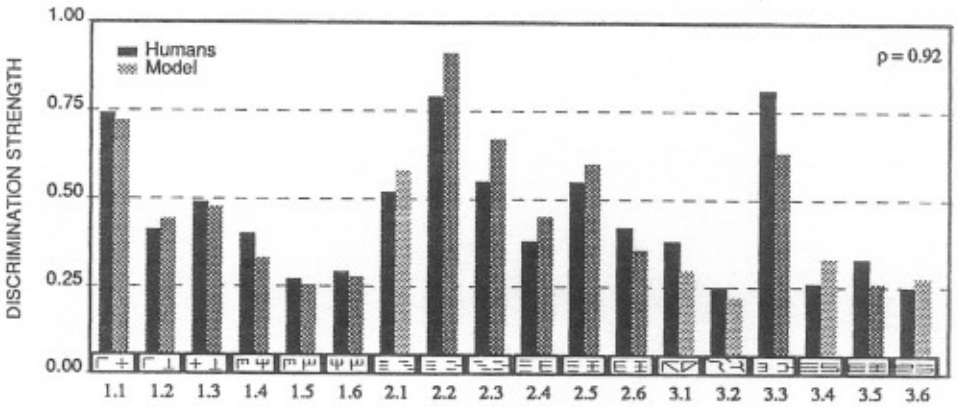


Figure 3: Model results Vs. human performance measured in psychophysical experiments. Human performance is due to Gurnsey and Browse

statistics, patterns with similar second order statistics were selected by an exhaustive search from this database of $10^4$ randomly generated patterns. This was done by an explicit computation and comparison of the dot distance distribution (neglecting the orientation since the patterns are randomly rotated). Figure 4 demonstrates two of these textures tested by the model. The left image consists of textures predicted to be almost indiscriminable (having almost identical symmetry measure in all locality channels). The right image consist of textures with similar second order statistics predicted to have some discriminability. Many other such examples were constructed and were verified qualitatively. Most predictions were found correct with few exceptions that may require more channels and further study. We suggest that a systematic and quantitative analysis of randomly generated patterns is indeed necessary for further evaluation of models and algorithms for texture discrimination.

While offering a better fit for psychophysical data than other computational models, our model should be viewed as part of a larger process. The generalized symmetry model may be a part of an hierarchical texture processing system in which the lowest level might compute simple Texton differences (orientation, size, color, brightness etc.) in low resolution; the next level quantifies local spatial relations based on local generalized symmetry; and the highest level may perform grouping processes as suggested by Beck [3]. In order to study and develop these ideas, a large scale stimuli database, constructed along the lines presented in this work, should be used for exhaustive analysis of new psychophysical, as well as computational, texture discrimination models.

## References


[1] J. Allman, F. Miezin, and E. McGuiness. Stimulus specific responses from beyond the classical receptive field. Ann. Rev. Neurosci., 8:407–430, 1985.

[2] J. Beck. Effect of orientation and of shape similarity on grouping. Percept. Psychophys., 1:300–302, 1966.

[3] J. Beck. Textural segmentation, Second order statistics, and Textural elements. Biol. Cybern., 48:125–130, 1983.

[4] J. R. Bergen and E. H. Adelson. Early vision and texture perception. Nature, 333:363–364, 1988.

[5] S. Edelman, D. Reisfeld, and Y.Yeshurun. Learning to recognize faces from examples. In Second European Conference on Computer Vision, S. Margherita, Ligure - Italy, May 1992.

[6] I. Fogel and D. Sagi. Gabor filters as texture descriminator. Biological Cybernetics, 61:103–113, 1989.

[7] R. Gurnsey and A. Browse. Micropattern properties and presentation conditions influencing visual texture discrimination. Percept. Psychophys., 41(3):239–252, 1987.

[8] Bela Julesz. Experiments in the visual perception of texture. Scientific American, 232:34–43, 1975.

[9] Bela Julesz. Textons, the elements of texture perception and their interactions. Nature, 290:91–97, 1981.

[10] Bela Julesz. Toward an axiomatic theory of preattentive vision. In Cowan WM Edelman GM, Gall WE, editor, Dynamic aspects of neocortical function, pages 585–612. Neurosciences Research Foundation, 1984.

[11] Bela Julesz. Texton gradients: The texton theory revisited. Biological Cybernetics, 54:245–251, 1986.

[12] B. J. Krose. Local structure analyzers as determinants of preattentive texture discrimination. Biol. Cybern., 55:289–298, 1987.

[13] E.H. Land and J. J. McCann. Lightness and retinex theory. J. Opt. Soc. Am., 61(1):1–11, 1971.

[14] J. Malik and P. Perona. Preattentive texture discrimination with early vision mechanisms. J. Opt. Soc. Am., 7(5):923–932, 1990.

[15] D. Reisfeld, H. Wolfson, and Y. Yeshurun. Detection of interest point using symmmetry. In Third International Conference on Computer Vision, pages 62–65, Osaka, Japan, December 1990.

[16] D. Reisfeld and Y. Yeshurun. Robust detection of facial features by generalized symmetry. In Proceedings of the 11th International Conference on Pattern Recognition, The Hague, Netherlands, September 1992.

[17] B. S. Rubenstein and D. Sagi. Spatial variability as a limiting factor in texture discrimination tasks: Implecations for performance asymmetries. Technical Report CS-89-12, The Weizmann institute of science, JULY 1989.

[18] Zucker S.W., Dobbins A., and Iverson L. Two stages of curve detection suggest two styles of visual computation. Neural Computation, 1:68–81, 1989.

[19] A. Triesman. Featursanalysis in early vision: evidence from search asymmetries. Psychological Review, 95:15–48, 1988.